

Wijngaard test around inclusions in microstructured solid and hollow core optical fibers

A. FAZACAS^{a,b}, P. STERIAN^{a,c}

^aAcademic Center for Optical Engineering and Photonics, Faculty of Applied Sciences, University “Politehnica” of Bucharest, 313 Splaiul Independentei, 060042 Bucharest, Romania

^bInstitute of Atomic Physics, Bucharest, Romania

^cAcademy of Romanian Scientists, 54 Splaiul Independentei, 050094 Bucharest, Romania

In this paper we describe the electromagnetic properties of modes in microstructured optical fibers (MOFs). It is well known that optical fibers have a large number of modes that can be used in different types of structures, at certain wavelengths. Also, multi-structural optical fibers have remarkable properties, namely: variable dispersion, nonlinearity, and single-mode operation over a wide range of wavelengths. We investigated the propagation of the electromagnetic modes, at different wavelengths in two types of MOFs: solid core fibers and hollow core fibers. Wijngaard stated that in a certain region, a field can be written as a superposition of outgoing waves from all source bodies. To describe the stability of the effective refractive index we used the Wijngaard test around inclusions in MOFs, we computed the Wijngaard integral W , which is a measure of the accuracy of the equality between the local and the Wijngaard expansions. Our simulations were made in CUDOS MOF Utilities software and are based on the multipole mathematical method.

(Received March 8, 2015; accepted May 7, 2015)

Keywords: Wijngaard test, Inclusions, Microstructured optical fibers, Solid core fibers, Hollow core fibers

1. Introduction

The study of electromagnetic properties in microstructured optical fibers (MOF) was of great interest lately, due to their ability to operate in single-mode over a wide range of wavelengths [1]. Also, these fibers have remarkable properties, as: large and adjustable dispersion and nonlinearity. Nonlinear microstructured fibers (made from lead oxide, bismuth oxide, tellurium oxide, and chalcogenide glasses) were designed for four-wave mixing - based telecommunication applications [2-4].

Boris et al. discussed a new transformation technique for analysing the wave vector content of microstructured optical fiber modes, to improve the efficiency in their computations. Also, this technique gives good physical insight into the nature of the mode [5].

The multipole method is a very powerful mathematical tool that was intensively used in the last decade, due to the increased computational efficiency in comparison with other methods [6-8]. The multipole method was used to: calculate the electromagnetic properties of the modes in microstructured optical fibers, calculate the air guided modes in photonic crystal fibers [9], analyse the photonic crystal fibers with coated inclusions [10].

In this study we simulated the electromagnetic modes for E_z component of the field in solid and hollow core fibers. Also, we performed a Wijngaard test around inclusions in MOFs, to describe the stability of the refractive index. For our simulation we used CUDOS MOF Utilities software.

2. Mathematical model

The term of holey fiber and microstructured optical fiber refer to any kind of fiber with a set of inclusions running along the fiber axis [11].

The geometry of the hollow and solid core fibers are presented in Fig. 1. For solid core fiber the geometry is similar to that of a conventional step index fiber, meaning that the refractive index in the cladding is smaller than the refractive index in the core. The wave-guide in solid core fiber is easier.

In the case of hollow core fibers the wavelength range is very narrow (few tens of nm for guidance in infrared and visible), making the guidance and the manufacture challenging.

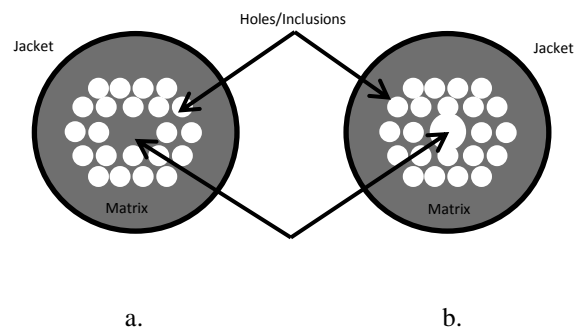


Fig. 1. a. Cross-section of a solid core microstructured optical fiber (SMOF); b. Cross-section of a hollow core microstructured optical fiber (HMOF).

Solid core and hollow core MOFs are both extremely promising new types of fibers, with completely different proprieties and possible applications [11].

The multipole method is a mathematical method to find the modes in step-index optical fiber and has numerous advantages: well suited for computation involving material dispersion, can be used over a wide range of wavelengths relative to MOF dimensions, can deal with solid core MOFs and air core photonic crystal fibers, the symmetrical proprieties permits the user to reduce the number of numerical computations [7, 8], [11].

The simplest model for the multipole method is that when we consider a single inclusion in the matrix (Fig. 2), with the center in the origin of the coordinate system [11, 12].

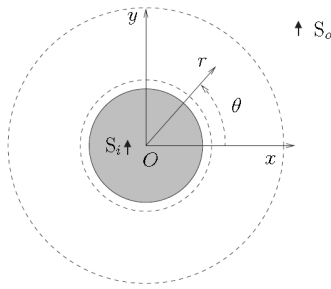


Fig. 2. Single inclusion in the matrix with the center in the origin where S_i and S_o are sources [9].

The field V can be written as a Fourier – Bessel series:

$$V(r, \theta) = \sum_{n \in \mathbb{Z}} \left(A_n J_n(k_{\perp}^M r) + B_n H_n^1(k_{\perp}^M r) \right) \exp(in\theta) \quad (1)$$

where $k_{\perp}^M r = \sqrt{k^2 n_M^2 - \beta^2}$ (k is the free space wave number, β the propagation constant, n_M the refractive index in the matrix); A_n, B_n Fourier-Bessel coefficients; J_n is the Bessel function of first kind of order n ; $H_n^1(k_{\perp}^M r) = J_n(k_{\perp}^M r) + iY_n(k_{\perp}^M r)$ is the Hankel function of first kind of order n ; Y_n is the Bessel function of second kind of order n .

Our Fourier-Bessel series can be split in two parts as we can see in equation (2): R – the regular part of V that describes the fields radiated from sources situated beyond the outer circle (S_o) and O – the singular part of V that describes the fields radiated from sources situated inside the inner circle (S_i). S_o radiates a field which is regular in the annulus and in the region delimited by the inner circle of the annulus, while S_i radiates a field that has a singularity in the annulus hence cannot be described by Fourier-Bessel series in that annulus [11,12].

$$\begin{aligned} V(r, \theta) &= R(r, \theta) + O(r, \theta) \\ R(r, \theta) &= A_n J_n(k_{\perp}^M r) \exp(in\theta) \\ O(r, \theta) &= B_n H_n^1(k_{\perp}^M r) \exp(in\theta) \end{aligned} \quad (2)$$

If we consider a complex case, then in the vicinity of the l^{th} (Fig. 3 where the solid lines indicate physical boundaries and the dashed lines indicate the regions of convergence) inclusion the electric field becomes [12]:

$$E_z = \sum_{m \in \mathbb{Z}} \left[A_m^{El} J_m(k_{\perp}^M r_l) + B_m^{El} H_m^1(k_{\perp}^M r_l) \right] \exp(im\theta_l) \quad (3)$$

where J_m is the incident part, while H_m^1 is the outgoing wave part. The equation is valid only from the surface of the cylinder to the nearest cylinder or source.

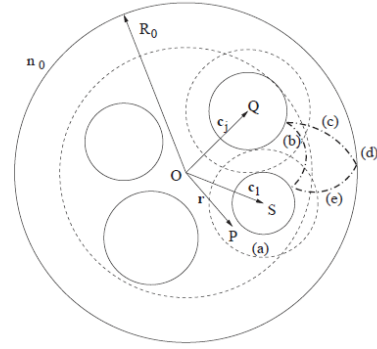


Fig. 3. Multiple inclusions in the matrix with the contributions to the fields outside a generic hole i [12].

Wijngaard describes in another way the fields, stating that a field in a region can be written as a superposition of outgoing waves from all sources bodies in the region:

$$\begin{aligned} E_z &= \sum_{l=1}^{N_i} \sum_{m \in \mathbb{Z}} B_m^{El} H_m^1(k_{\perp}^M |r_l|) e^{im \arg(r-c_j)} + \\ &+ \sum_{m \in \mathbb{Z}} A_m^{E0} J_m(k_{\perp}^M r) e^{im\theta} \end{aligned} \quad (4)$$

Equation (4) is valid everywhere in the matrix. By combining equations (3) and (4) we obtain:

$$\begin{aligned} \sum_{m \in \mathbb{Z}} A_m^{El} J_m(k_{\perp}^M r_l) e^{im\theta_l} &= \sum_{\substack{j=1 \\ j \neq l}}^{N_i} \sum_{m \in \mathbb{Z}} B_m^{Ej} H_m^1(k_{\perp}^M r_j) e^{im\theta} + \\ &+ \sum_{m \in \mathbb{Z}} A_m^{E0} J_m(k_{\perp}^M r) e^{im\theta} \end{aligned} \quad (5)$$

where the sum on the left hand side is associated with the regular incident field for inclusion l , while the double sum on the right hand side is associated with the outgoing field originating from all other inclusions ($j \neq l$), and the last sum represents the field coming from the jacket [12,13].

We conclude that:

$$E_z = V_j + V_{inc} \quad (6)$$

where the term V_j is generated by sources placed inside or at the boundary of the j^{th} inclusion, while the term V_{inc} is generated by sources outside or on the jacket boundary.

Through the Wijnngaard integral we describe the stability of the effective refractive index with respect to increase of multipole order. The Wijnngaard integral is a measure of the accuracy of the equality between the local (eq. 3) and the Wijnngaard expansions (eq. 4) and is defined as [8]:

$$W = \frac{\int_{C1} |E_z^{local}(\theta_1) - E_z^{Wijnngaard}(\theta_1)| d\theta_1}{\int_{C1} |E_z^{Wijnngaard}(\theta_1)| d\theta_1} \quad (7)$$

3. Simulated results and discussions

First, we consider a hollow core fiber with the following parameters: the number of the rings is equal with 3, the number of the missing rings is equal with 2, the central cylinder radius is equal with $5,55 \mu\text{m}$, the cylinder radius is equal to $1,75 \mu\text{m}$ and d/pitch is equal to 2,22.

In Fig. 4 we illustrated the real part, the imaginary part and the calculated Bloch modes for different wavelengths inside the hollow core fiber.

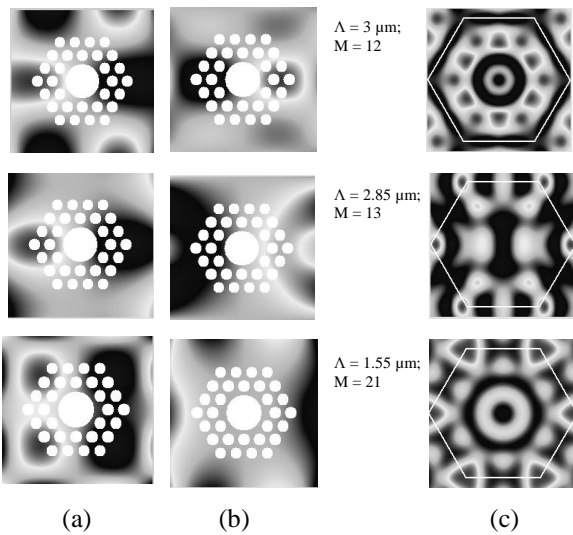


Fig. 4. Normalized real (a) and imaginary (b) field E_z for HMOF; (c) The computed Bloch Transform.

In Fig. 5 we illustrated the evolution of the local field (dashed line) in comparison with the evolution of the field resulting from the Wijnngaard expansion (solid line) for different multipole (M) order in hollow core fibers. We observed that for $M = 1$, the local field and the Wijnngaard field have different evolutions, while for $M = 9$ and $M = 12$ the evolution of the two fields are almost similar. Consequently, for $M = 1$ the effective refractive index is unstable, while for $M = 12$ the effective refractive index is stable.

The magnitude difference between the local field and the field resulting from the Wijnngaard expansion for different wavelengths is presented in Fig. 6.

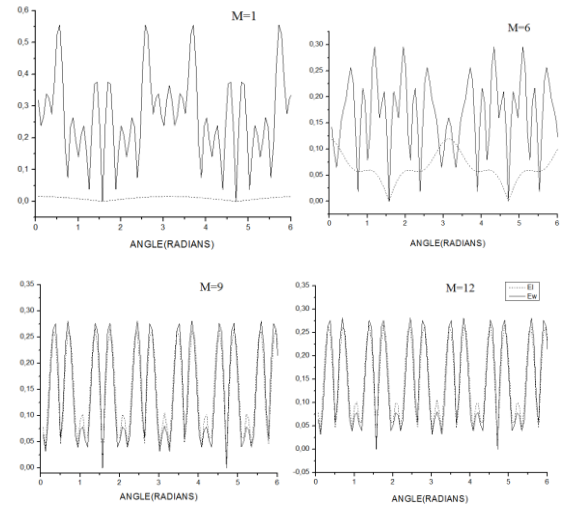


Fig. 5. The evolution of the local field and the field resulting from the Wijnngaard expansion for different multipole orders – HMOF.

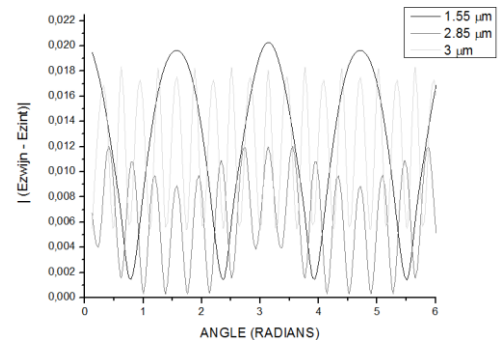


Fig. 6. The magnitude difference between the local field and the field resulting from the Wijnngaard expansion for different wavelengths – HMOF.

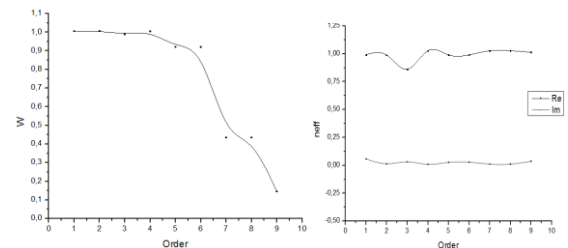


Fig. 7. The evolution of the Wijnngaard integral and the evolution of the refractive index with the multipole order.

The evolution of the Wijnngaard integral and the evolution of the refractive index with the multipole order are presented in Fig. 7. We observed that the Wijnngaard integral decreases with the increase of the multipole orders. Also, as the multipole order increases, the effective

refractive index stabilizes, around 0,97 for the real part and around 0,01 for the imaginary part.

Next, we consider a solid core fiber with the following parameters: the number of the rings is equal with 3, the number of the missing rings is equal with 2, the cylinder radius is equal to $1,75 \mu\text{m}$ and d/pitch is equal to 0,70.

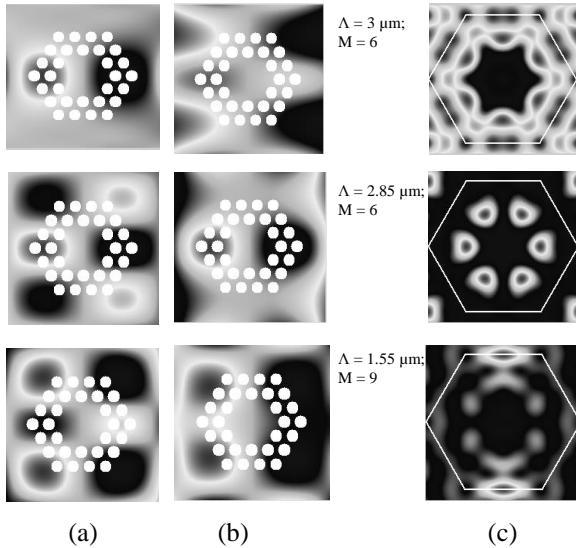


Fig. 8. Normalized real (a) and imaginary (b) field E_z for SMOF; (c) The computed Bloch Transform.

Fig. 9 illustrates the evolution of the local field (dashed line) in comparison with the evolution of the field resulting from the Wijngaard expansion (solid line) for different multipole (M) orders in solid core fibers. For $M = 1$ and $M = 3$ the evolution of the local field and the evolution of the Wijngaard field were different. We observed that for $M = 5$ the refractive index is very stable.

In Fig. 10 we illustrated the difference between the local field and the field resulting from the Wijngaard expansion for different wavelengths.

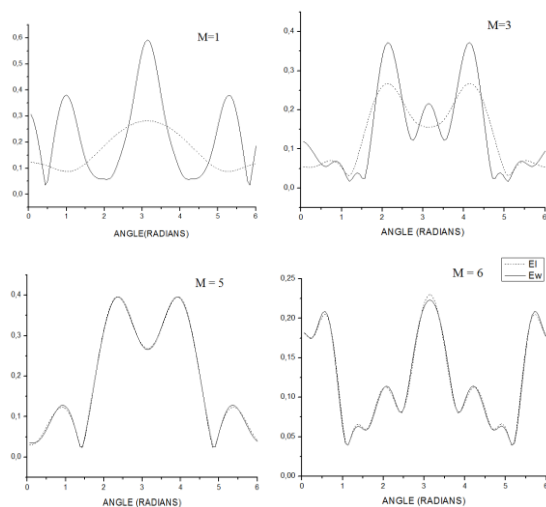


Fig. 9. The evolution of the local field and the field resulting from the Wijngaard expansion for different multipole orders – SMOF.

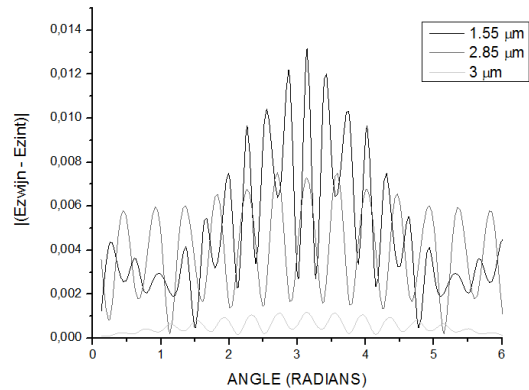


Fig. 10. The magnitude difference between the local field and the field resulting from the Wijngaard expansion for different wavelengths – SMOF.

As in the previous case, the evolution of the Wijngaard integral and the evolution of the refractive index with the multipole order are presented in Fig. 11. In the case of the solid core fibers we observed that the Wijngaard integral decreases with the increase of the multipole order. Also, as the multipole order increases, the effective refractive index stabilizes, around 0,99 for the real part and around 0,04 for the imaginary part.

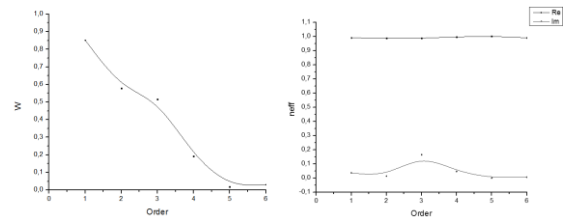


Fig. 11. The evolution of the Wijngaard integral and the evolution of the refractive index with the multipole order.

4. Conclusions

This paper describes some of the electromagnetic properties of modes in solid and hollow core MOFs. The stability of the effective refractive index is an important parameter in MOFs design.

By using CUDOS MOF Utilities software we demonstrated that for solid and hollow core MOFs the Wijngaard integral decreases with the increase of the multipole order. Consequently, the effective refractive index stabilizes with the decrease of the Wijngaard integral.

References

- [1] H. P. Uranus, H. J. W. M. Hoekstra, E. van Groesen, Proceedings Symposium IEEE/LEOS Benelux Chapter, Ghent (2004).
- [2] Jiri Kanka, Photonic Crystal Fibers II, Proc. of SPIE 6990, 69900E (2008).

- [3] A. A. Popescu, R. Savastru, D. Savastru, et al., *Digest Journal of Nanomaterials and Biostructures*, **6**(3), 1245 (2011).
- [4] A. R. Sterian, Hindawi Publishing Corporation, *Advances in High Energy Physics*, **2073**, Article ID 516396, 8 (2013).
- [5] Boris T. Kuhlmeiy, Ross C. McPhedran, C. Martijn de Sterke, *Optics Express*, **12**(8), 1769 (2004).
- [6] A. R. Sterian, *Computational Science and Its Applications - ICCSA 2007, Pt 1, Proceedings Book Series: LECTURE NOTES IN COMPUTER SCIENCE* **4705**, 436 (2007).
- [7] T. P. White, B. T. Kuhlmeiy, R. C. McPhedran, D. Maystre, G. Renversez, C. Martijn de Sterke, L. C. Botten, *J. Opt. Soc. Am. B*/**19**(10), (2002).
- [8] Boris T. Kuhlmeiy, Thomas P. White, Gilles Renversez, Daniel Maystre, Lindsay C. Botten, C. Martijn de Sterke, Ross C. McPhedran, **19**(10), *J. Opt. Soc. Am. B.*, (2002).
- [9] T. P. White, R. C. McPhedran, L. C. Botten, G. H. Smith, C. Martijn de Sterke, *Optics Express*, **9**(13), 721 (2001).
- [10] Boris T. Kuhlmeiy, Karrnan Pathmanandavel, Ross C. McPhedran, *Optics Express*, **14**(22), 10851 (2006).
- [11] Frédéric Zolla, Gilles Renversez, André Nicolet, Boris Kuhlmeiy, Sébastien Guenneau, Didier Felbacq, *Foundations of Photonic Crystal Fibers*, Imperial College Press, London, (2005).
- [12] F. C. Maciuc, et al., *ROMOPTO 2000: SIXTH Conference on Optics, Proc. SPIE*, **4430**, 136 (2000).
- [13] Thomas Grujic, Boris T. Kuhlmeiy, C. Martijn de Sterke, Chris G. Poulton, *Journal of the Optical Society of America B*, **26**(10), 1852 (2009).

*Corresponding author: a.fazacas@ifm-mg.ro